Title

Myeloid-Cell-Derived VEGF Maintains Brain Glucose Uptake and Limits Cognitive Impairment in Obesity

Journal

Cell, 165(4)

ISSN

0092-8674

Authors

Jais, Alexander
Solas, Maite
Backes, Heiko
et al.

Publication Date

2016-05-01

DOI

10.1016/j.cell.2016.03.033

Peer reviewed

Article

Cell

Myeloid-Cell-Derived VEGF Maintains Brain Glucose Uptake and Limits Cognitive Impairment in Obesity

Graphical Abstract

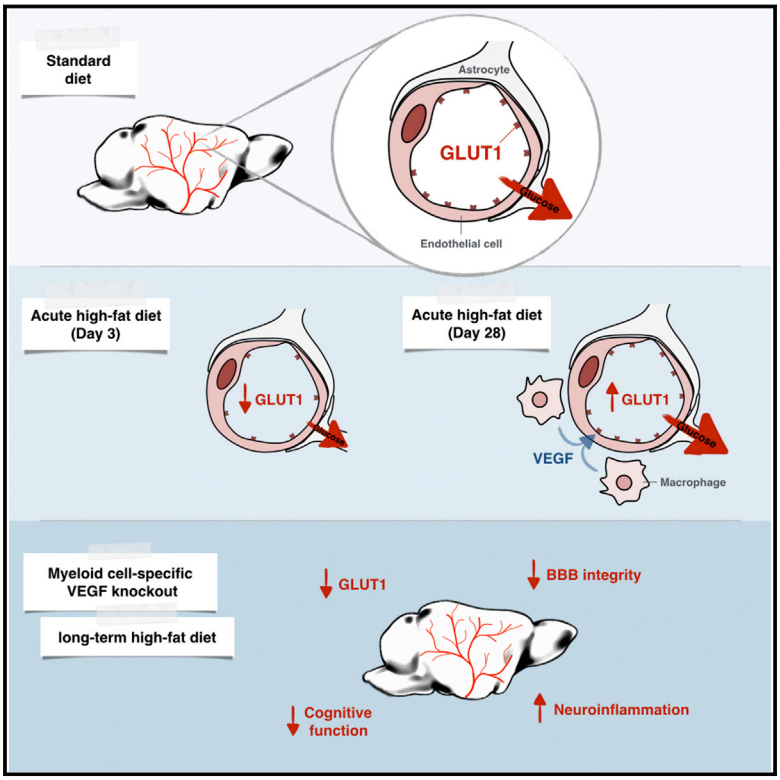

Highlights

- Acute high-fat feeding suppresses GLUT1 expression at the blood-brain barrier (BBB)
- Macrophages at the BBB increase VEGF expression upon prolonged HFD feeding
- Inducible GLUT1 deletion in brain endothelial cells leads to increased VEGF secretion
- Myeloid-cell-specific disruption of VEGF impairs cognitive function in obesity

Authors

Alexander Jais, Maite Solas, Heiko Backes, ..., Napoleone Ferrara, Gerard Karsenty, Jens C. Brüning

Correspondence

bruening@sf.mpg.de

In Brief

Acute high-fat feeding suppresses brain glucose uptake. To preserve cognitive function after prolonged feeding on a high-fat diet and to forestall neurodegeneration in obesity, there is a compensatory upregulation of glucose transporters at the blood-brain barrier as a result of inflammatory signals from perivascular macrophages.

Jais et al., 2016, Cell *165*, 882–895
May 5, 2016
http://dx.doi.org/10.1016/j.cell.2016.03.033

CellPress

Cell

Article

Myeloid-Cell-Derived VEGF Maintains Brain Glucose Uptake and Limits Cognitive Impairment in Obesity

Alexander Jais,[1,2,3,11] Maite Solas,[1,2,3,11] Heiko Backes,[1] Bhagirath Chaurasia,[1] André Kleinridders,[1,4,5] Sebastian Theurich,[1,2,3] Jan Mauer,[1,2,3] Sophie M. Steculorum,[1,2,3] Brigitte Hampel,[1,2,3] Julia Goldau,[1,2,3] Jens Alber,[1,2,3] Carola Y. Förster,[6] Sabine A. Eming,[3,7] Markus Schwaninger,[8] Napoleone Ferrara,[9] Gerard Karsenty,[10] and Jens C. Brüning[1,2,3,5,*]

[1]Department of Neuronal Control of Metabolism, Max Planck Institute for Metabolism Research, Gleueler Strasse 50, 50931 Cologne, Germany

[2]Center for Endocrinology, Diabetes and Preventive Medicine (CEDP), University Hospital Cologne, 50924 Cologne, Germany

[3]Excellence Cluster on Cellular Stress Responses in Aging Associated Diseases (CECAD) and Center of Molecular Medicine Cologne (CMMC), University of Cologne, Joseph Stelzmann Strasse 26, 50931 Cologne, Germany

[4]German Institute of Human Nutrition Potsdam-Rehbruecke, Central Regulation of Metabolism, Arthur-Scheunert-Allee 114-116, 14558 Nuthetal, Germany

[5]National Center for Diabetes Research (DZD), Ingolstädter Land Strasse 1, 85764 Neuherberg, Germany

[6]Department of Anaesthesia and Critical Care, University of Würzburg, Oberdürrbacher Strasse 6, 97080 Würzburg, Germany

[7]Department of Dermatology, University of Cologne, 50937 Cologne, Germany

[8]Institute of Experimental and Clinical Pharmacology and Toxicology, University of Lübeck, Ratzeburger Allee 160, 23562 Lübeck, Germany

[9]Moores Cancer Center, University of California, 3855 Health Sciences Drive, La Jolla, CA 92093, USA

[10]Department of Genetics and Development, Columbia University, 701 West 168th Street, New York, NY 10032, USA

[11]Co-first author

*Correspondence: bruening@sf.mpg.de

http://dx.doi.org/10.1016/j.cell.2016.03.033

SUMMARY

High-fat diet (HFD) feeding induces rapid reprogramming of systemic metabolism. Here, we demonstrate that HFD feeding of mice downregulates glucose transporter (GLUT)-1 expression in blood-brain barrier (BBB) vascular endothelial cells (BECs) and reduces brain glucose uptake. Upon prolonged HFD feeding, GLUT1 expression is restored, which is paralleled by increased expression of vascular endothelial growth factor (VEGF) in macrophages at the BBB. In turn, inducible reduction of GLUT1 expression specifically in BECs reduces brain glucose uptake and increases VEGF serum concentrations in lean mice. Conversely, myeloid-cell-specific deletion of VEGF in VEGF$^{\Delta myel}$ mice impairs BBB-GLUT1 expression, brain glucose uptake, and memory formation in obese, but not in lean mice. Moreover, obese VEGF$^{\Delta myel}$ mice exhibit exaggerated progression of cognitive decline and neuroinflammation on an Alzheimer's disease background. These experiments reveal that transient, HFD-elicited reduction of brain glucose uptake initiates a compensatory increase of VEGF production and assign obesity-associated macrophage activation a homeostatic role to restore cerebral glucose metabolism, preserve cognitive function, and limit neurodegeneration in obesity.

INTRODUCTION

Over the last years, it has become evident that homeostatic signals, as exemplified by leptin (Zhang et al., 1994), communicate energy storage of the organism to the brain to adapt behavioral and autonomic responses in control of energy homeostasis (Gautron et al., 2015; Kleinridders et al., 2009a). Importantly, high-fat diet (HFD) feeding can cause a state of neuronal leptin and insulin resistance to promote positive energy balance (Vogt and Brüning, 2013; Williams and Elmquist, 2012). Here, the manifestation of neuronal insulin and leptin resistance has been linked to the activation of inflammatory signaling cascades, similar to what is observed in peripheral metabolic tissues, such as liver, skeletal muscle, and adipose tissue of obese animal models and humans (Gregor and Hotamisligil, 2011; Kleinridders et al., 2009b; Tsaousidou et al., 2014). However, the exact mechanism(s) of how inflammatory signaling cascades are activated in obesity remain only partly defined. In this respect, it is remarkable how rapidly shifting animals to high-fat-containing, energy-dense food reprograms metabolism and concomitantly regulates inflammation. Within only 3 days of HFD feeding, expression of proinflammatory cytokines increases in the hypothalamus of rodents as the key regulatory center in energy and glucose homeostasis (Thaler et al., 2012). These acute changes are later accompanied by a whole array of cellular responses, including gliosis,

alterations in brain vasculature, and blood-brain barrier (BBB) integrity (Kälin et al., 2015; Thaler et al., 2012; Yi et al., 2012a, 2012b). Despite all this knowledge on the acute effects of altered nutrition and acutely shifting systemic metabolism to fat utilization, the consequences of this intervention for the brain as an organ critically depending on sustained energy supply, covered primarily by glucose metabolism, remain largely undefined.

Glucose uptake—also in the CNS—occurs primarily by facilitated diffusion through a family of specific glucose transporters. Glucose transporter 1 (GLUT1), encoded by *SLC2A1*, is the predominant glucose transporter expressed on vascular endothelial cells of the BBB (Takata et al., 1990). Alterations of GLUT1 expression have severe consequences, underlining the critical importance of this transporter to ensure glucose uptake in the brain in addition to further roles in other tissues (Freemerman et al., 2014; Heilig et al., 2003; Macintyre et al., 2014; Wang et al., 2006). Thus, homozygous inactivation of the *Slc2a1* gene in mice leads to embryonic lethality (Wang et al., 2006). Already, heterozygous *Slc2a1* knockout mice exhibit impaired motor function as well as spontaneous seizures, therefore mimicking the major features of the human GLUT1-deficiency syndrome (GLUT1-DS), where haploinsufficiency of the *SLC2A1* gene is the cause of a rare form of encephalopathy (Wang et al., 2006). Here, the functional deficiency of the GLUT1 protein limits brain glucose availability and is characterized by infantile seizures, developmental delay, and acquired microcephaly (De Vivo et al., 1991; Seidner et al., 1998). Recently, it was shown that GLUT1 is of paramount importance for maintenance of capillary networks, blood flow, and BBB integrity, and reductions in GLUT1 levels contribute to neuronal dysfunction and neurodegeneration in mice (Winkler et al., 2015). In individuals with Alzheimer's disease (AD), GLUT1 expression at the BBB has been reported to decrease (Horwood and Davies, 1994; Kalaria and Harik, 1989; Mooradian et al., 1997; Vannucci et al., 1994). However, the GLUT1-dependent regulation of brain glucose uptake in obesity has so far not been directly addressed.

In order to define the potential acute HFD feeding-elicited changes in cerebral glucose metabolism, we examined the regulation of brain glucose transporters in response to HFD feeding. We find that GLUT1 expression decreases in response to HFD feeding, leading to transiently decreased brain glucose uptake. Upon prolonged HFD feeding, GLUT1 expression is restored in brain endothelial cells (BECs), which is paralleled by increased recruitment and VEGF expression of perivascular macrophages and increased circulating VEGF concentrations. In turn, short-term treatment of mice with recombinant vascular endothelial growth factor (VEGF) can prevent the acute brain glucose uptake-inhibitory effect of HFD feeding. Genetically mimicking partial, acute reduction of GLUT1-BBB expression similarly reduces brain glucose uptake and evokes a compensatory increase in circulating VEGF concentrations. Moreover, myeloid-cell-specific ablation of VEGF in mice reduces BBB-GLUT1 expression, brain glucose uptake, memory formation, and aggravates AD progression in obese but not in lean mice. Collectively, our experiments reveal a critical role for VEGF and HFD-elicited activation of inflammation to ensure cerebral glucose metabolism and to limit progression of neurodegeneration in obesity.

RESULTS

Acute HFD Feeding Impairs Brain Glucose Uptake

Acute HFD feeding rapidly reprograms systemic metabolism and fuel usage (Lee et al., 2011; Thaler et al., 2012). This notion was further substantiated when we assessed systemic substrate usage via indirect calorimetry in mice upon acutely switching feeding from normal chow diet (NCD) to high-fat diet (HFD). Metabolism under these conditions acutely shifts from circadian, alternating carbohydrate and fat usage to a permanent predominance of fat utilization, a phenomenon that is accompanied by rapid weight gain and increased glycemia (Figures 1A, S1A, and S1B). We next aimed to investigate how cerebral glucose metabolism acutely adapts to HFD feeding and its accompanying alterations in systemic substrate usage. To this end, we first compared the mRNA expression of critical glucose transporters in the CNS of mice, which had either remained on NCD feeding or had been switched to HFD feeding for 3 days. This analysis revealed a dramatic 50% downregulation of *Slc2a1* expression, while expression of *Slc2a3* and *Slc2a5* remained unaltered (Figure 1B). When we further assessed the dynamics of brain *Slc2a1* expression upon acute HFD feeding, we found that brain *Slc2a1* mRNA expression was transiently reduced as early as 3 days of HFD feeding and remained suppressed until 1 week of HFD feeding, while it slowly recovered 2 weeks after HFD feeding initiation and was restored to comparable extend to that observed in constantly NCD fed animals after 4 weeks of HFD feeding (Figure 1C).

Next, we directly assessed GLUT1 protein expression in BECs via immunofluorescent staining for endothelial-cell-specific lectin and GLUT1. GLUT1 immunoreactivity was significantly reduced in BECs between 3 and 7 days after HFD feeding initiation (Figures 1D and S1C). Taken together, these experiments clearly indicate that acute HFD feeding transiently reduces the expression of the critical glucose transporter for brain glucose uptake, i.e., GLUT1 at the BBB.

In order to investigate potential compensatory mechanisms, which could account for restoration of GLUT1 expression upon prolonged HFD feeding, we monitored circulating VEGF concentrations, as VEGF is able to upregulate GLUT1 expression at the blood-brain barrier (Lee et al., 2007; Mani et al., 2003; Pekala et al., 1990; Sone et al., 2000; Yeh et al., 2008). Assessment of circulating VEGF concentrations revealed significantly increased serum VEGF concentrations 4 weeks after initiation of HFD feeding, concomitant with full restoration of BBB-GLUT1 expression at this time (Figure 1E). To investigate the origin of increased VEGF production upon HFD feeding, we monitored *Vegfa* mRNA expression in spleen, liver, and adipose tissue at different times of HFD feeding. This analysis revealed that *Vegfa* mRNA expression only transiently increased in the spleen 7 days after initiation of HFD feeding (Figures S1D–S1F). However, this transient upregulation clearly cannot account for the prolonged increase in circulating VEGF concentrations and potentially the prolonged restoration of BBB-GLUT1 expression upon chronic HFD feeding.

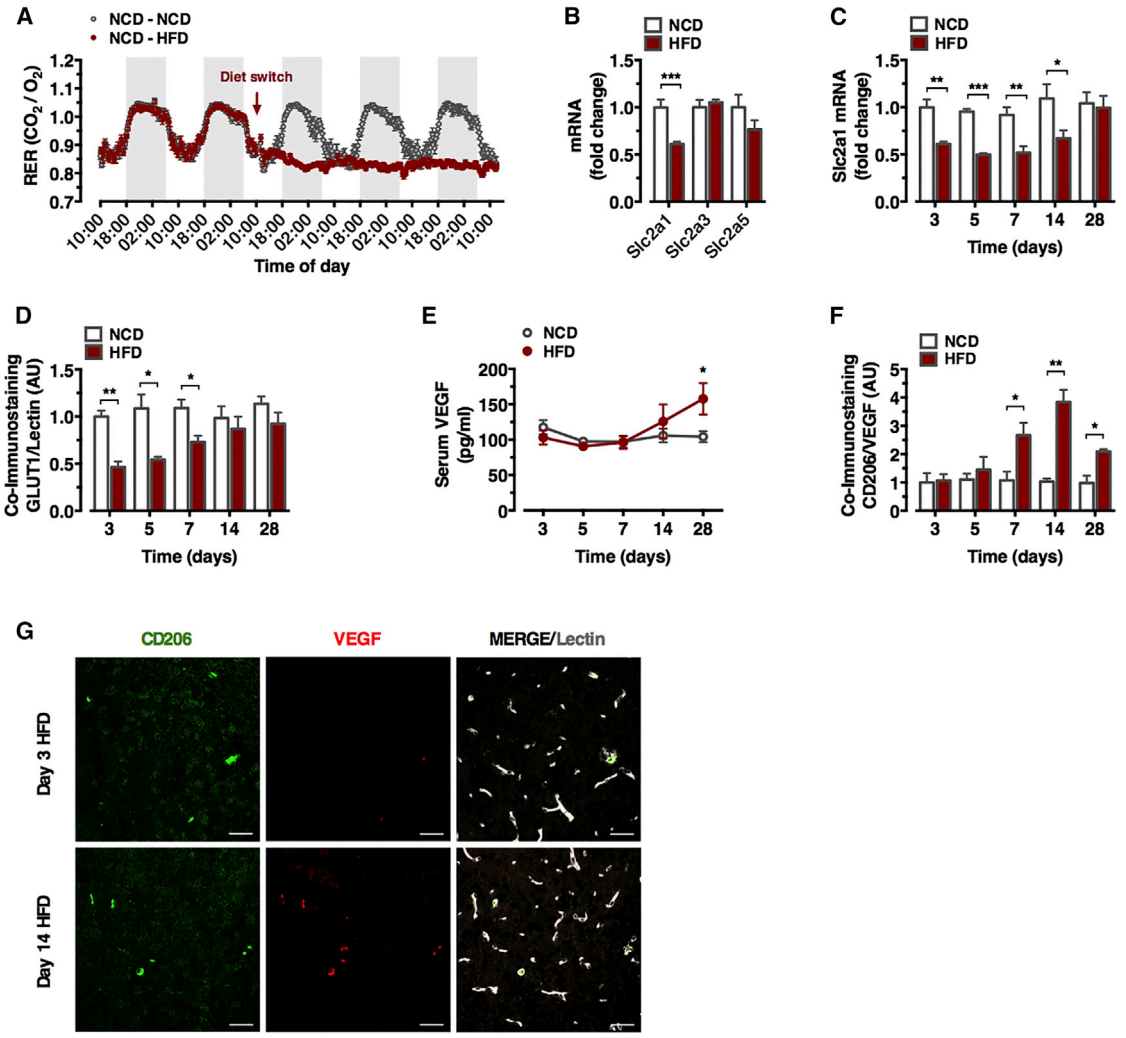

Figure 1. High-Fat Diet Acutely Downregulates GLUT1 in BECs

(A) Respiratory exchange rate (RER) of 8-week-old C57BL/6N mice switched to high-fat diet (HFD) or remained on normal chow diet (NCD). Grey bars denote dark phases; n = 8 per group.

(B) qPCR analysis of glucose transporter mRNA in cortical brain samples, n = 5 per group.

(C) qPCR analysis of *Slc2a1* (GLUT1) mRNA in the cortical brain during acute HFD, n = 5 per group.

(D) Quantification of co-immunostaining of GLUT1 and lectin on cortical brain sections, n = 5 per group.

(E) Serum VEGF levels during acute NCD/HFD feeding, n = 9/10 per group.

(F) Quantification of co-immunostaining of CD206 and VEGF on cortical brain sections, n = 3 per group.

(G) Representative confocal microscope analysis of CD206 (green), VEGF (red), and lectin-positive capillaries (white) on cortical brain sections. Scale bar, 50 μm.

Results presented as mean ± SEM. *p < 0.05, **p < 0.01, ***p < 0.001.

See also Figure S1.

Since CD206-positive macrophages are a rich source of VEGF production (He et al., 2012), we next assessed the abundance of these cells at the BBB and their VEGF immunoreactivity at different times following initiation of HFD feeding. Both the number and VEGF immunoreactivity of perivascular, CD206-positive macrophages increased as early as 5 days after HFD feeding, increased constantly until 14 days after HFD feeding initiation, and was persistently elevated up to 28 days into HFD feeding (Figures 1F, 1G, and S1G).

Next, we aimed to directly investigate whether acute HFD feeding indeed reduced brain glucose uptake as suggested by reduced BBB-GLUT1 mRNA and protein expression. To this end, we employed ^{18}F-FDG positron emission tomography (PET) scans to quantitatively assess brain glucose uptake. Therefore, wild-type animals were subjected to ^{18}F-FDG PET scans and thereafter either remained on NCD or switched to HFD for 3 days. After 3 days, the ^{18}F-FDG PET scan was repeated and brain glucose uptake was compared to the baseline scan of the same animals. While repeated ^{18}F-FDG PET scans in animals, which remained on NCD, expectedly revealed no decrease in brain glucose uptake (Figures S2A–S2D), animals that were placed on HFD for 3 days exhibited significantly

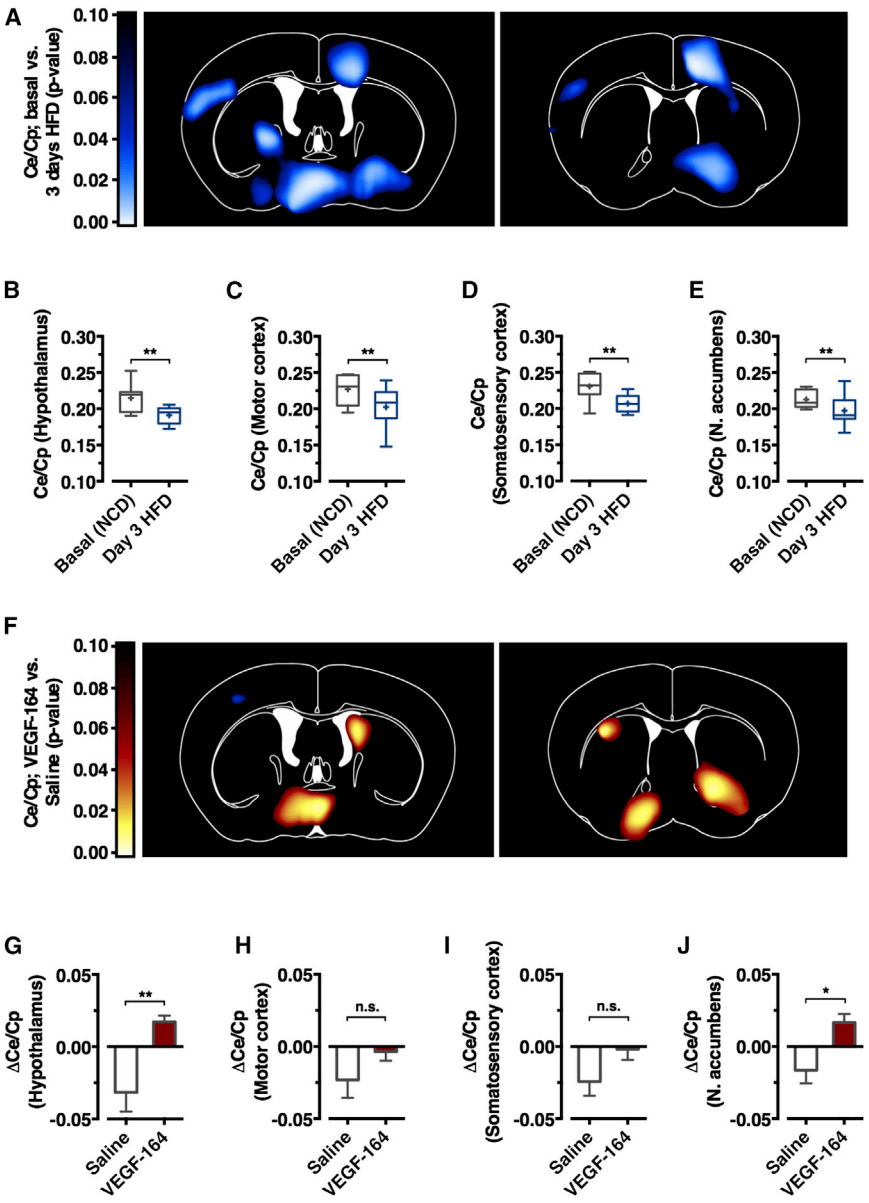

Figure 2. High-Fat Diet Acutely Downregulates Brain Glucose Uptake In Vivo

(A) Images showing differential regional glucose uptake in animals before and three days after exposure to HFD. Color code represents the p value for the indicated voxels in a paired Student's t test before and after diet exposure for nine animals. Reductions in glucose uptake are shown in blue color.

(B–E) Quantification of brain glucose uptake before and 3 days after HFD-exposure in nine animals in the hypothalamus (B), motor cortex (C), somatosensory cortex (D), and nucleus accumbens (E). Data were analyzed using a paired Student's t test.

(F) Differential regional glucose uptake in animals treated with recombinant VEGF-164 or with saline (n = 8/9) while exposed to HFD for 3 days. Increase in glucose uptake is shown in red color, decrease in blue color.

(G–J) Quantification of changes in glucose uptake in VEGF-164 and saline-treated animals (n = 8/9) in the hypothalamus (G), motor cortex (H), somatosensory cortex (I), and nucleus accumbens (J). Results presented as mean ± SEM or as box plots. Upper and lower whiskers indicate the minimum and maximum values of the data, centerlines indicate the median and the mean values are represented by plus signs. *$p < 0.05$, **$p < 0.01$. See also Figure S2.

reduced glucose uptake in motor and sensory cortex, hypothalamus, and nucleus accumbens compared to their baseline scan (Figures 2A–2E), revealing that diet-induced reduction of GLUT1 expression also functionally translated in reduced brain glucose uptake.

To investigate whether the restored GLUT1 expression observed upon prolonged HFD feeding also translated into a functional restoration of brain glucose uptake in these mice, we investigated another cohort of mice, in which serial ^{18}F-FDG PET scans were performed before onset of HFD feeding, as well as 3 and 21 days after HFD feeding. This analysis confirmed the robust suppression of brain glucose uptake in mice fed HFD for 3 days, but failed to detect a significant reduction of brain glucose uptake in mice fed a HFD for 21 days compared to the baseline scan under NCD feeding (Figures S2E–S2H).

To test whether VEGF can indeed counteract the HFD feeding-induced suppression of brain glucose uptake, we performed a rescue experiment, where mice were injected twice daily either with saline or recombinant VEGF during an acute 3-day exposure to HFD feeding, followed by ^{18}F-FDG PET scans. This treatment increased serum VEGF concentrations comparable to those observed in wild-type mice fed HFD for 4 weeks (Figures 1E and S2I). Glucose uptake in the VEGF-treated mice returned back to baseline levels in the cortex and even increased in the hypothalamus and the nucleus accumbens (Figures 2F–2J) compared to saline-injected control mice.

Saturated Fatty Acids Suppress BBB-GLUT1 Activity

In order to identify potential mediators of HFD-induced downregulation of BBB-GLUT1 expression, we first investigated whether serum of animals, which were exposed to HFD for 3 days, contained factors capable of decreasing GLUT1 expression in BECs. To this end, we incubated immortalized BECs for 24 hr with serum of mice, which were kept on NCD or fed an HFD for 3 days. qPCR analysis revealed a robust 90% reduction of *Slc2a1* mRNA expression upon incubation with HFD serum (Figure 3A). Similarly, GLUT1 protein expression was robustly repressed by incubating BECs with serum of short-term HFD fed mice (Figure 3B).

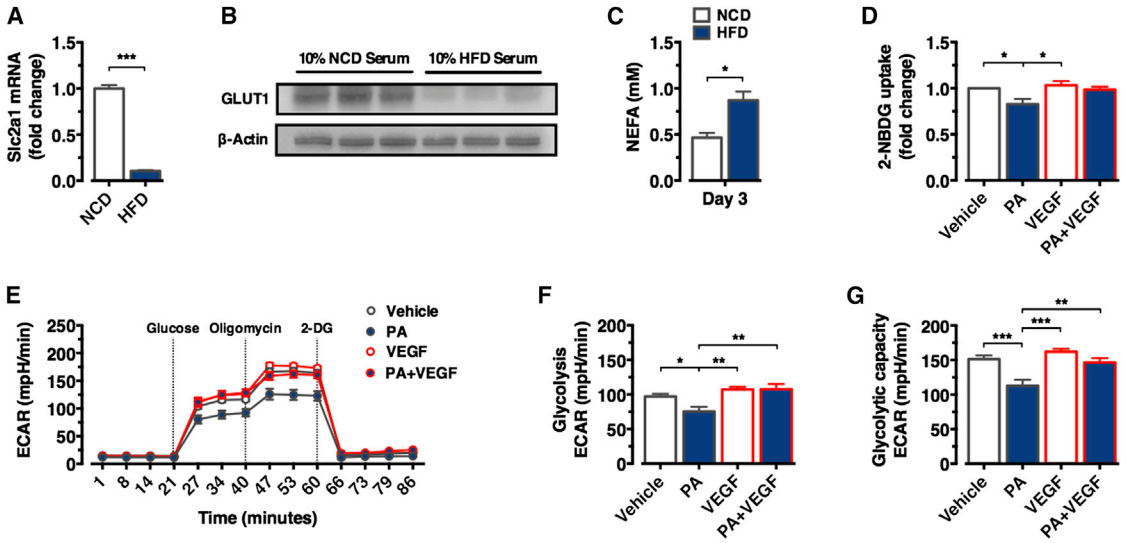

Figure 3. Serum of HFD-Fed Mice and Palmitic Acid Acutely Suppresses Glucose Uptake in Cultured BECs

(A) qPCR analysis of *Slc2a1* mRNA expression in cultured BECs, which had been cultured for 24 hr in the presence of 10% serum obtained from mice fed NCD or exposed to HFD for 3 days. Data represent the mean ± SEM of four BEC cultures in each group, each incubated with serum from different NCD/HFD-fed mice.

(B) GLUT1 protein expression in cultured BECs, which had been cultured for 24 hr in the presence of 10% serum obtained from mice fed NCD or exposed to HFD for 3 days as assessed by western blot analysis. Each lane represents lysates of BECs, which had been incubated with pooled serum of three different NCD- or three different HFD-fed mice.

(C) Comparative analysis of serum NEFA concentrations of mice fed NCD or after 3 days of HFD feeding. Data represent the mean ± SEM of six independent mice under each condition.

(D) Glucose uptake analysis using 2-NBDG. Data represent the mean ± SEM of three independent experiments.

(E) Glycolytic flux analysis of cultured BECs, incubated with 600 μM of palmitic acid and/or 100 ng/ml of recombinant VEGF. A representative result from three independent experiments is shown. n = 12 per group.

(F and G) Quantification of glycolysis (F) and glycolytic capacity (G) as described in (E).

Results presented as mean ± SEM. *p < 0.05, **p < 0.01, ***p < 0.001.

Next, we hypothesized that altered lipid composition of serum of HFD-fed mice might contribute to its ability to decrease glucose uptake in BECs. We analyzed the serum content of non-esterified fatty acids (NEFAs) of mice kept on either NCD or fed an HFD for 3 days. This analysis revealed an increase of NEFA serum concentrations in HFD-fed mice (Figure 3C). Therefore, we assessed whether saturated fatty acids might functionally impair glucose uptake and subsequent glycolysis in BECs. Indeed, incubating these cells with palmitic acid resulted in decrease of glucose uptake (Figure 3D) and glycolytic flux (Figures 3E–3G). Furthermore, we found that recombinant VEGF could prevent palmitic acid-induced suppression of glucose uptake and glycolysis in these cells (Figures 3D–3G).

Inducible GLUT1 Deletion in BECs Reduces Brain Glucose Uptake and Increases Circulating VEGF Concentrations

In order to investigate whether reducing GLUT1 expression to similar extend as observed upon acute HFD feeding reduces brain glucose uptake and potentially elicits a compensatory increase in circulating VEGF concentrations, we aimed to genetically reduce expression of GLUT1 specifically in BECs of adult mice. To this end, we crossed mice that carry a loxP-flanked *Slc2a1* allele (Wei et al., 2015) with those expressing a CreERT2-fusion protein under control of the thyroxine transporter *Slco1c1*-promoter specifically in BECs (Ridder et al., 2011), thus allowing for BEC-specific, tamoxifen-inducible deletion of GLUT1. To investigate the consequences of acute, dose-dependent reduction of GLUT1 expression in BECs, we used both mice heterozygous for the floxed *Slc2a1* allele (*Slc2a1*$^{lox/+}$ *Slco1c1*-CreERT2$^{+/-}$, i.e., GLUT-1$^{i\Delta/+BBB}$ mice) as well as those homozygous for the *Slc2a1* floxed allele (*Slc2a1*$^{lox/lox}$ *Slco1c1*-CreERT2$^{+/-}$, i.e., GLUT-1$^{i\Delta BBB}$ mice). After tamoxifen treatment for 3 days, brain cortices of control, GLUT-1$^{i\Delta/+BBB}$ mice, and GLUT-1$^{i\Delta BBB}$ mice were analyzed for *Slc2a1* expression via qPCR and by co-immunohistochemistry for GLUT1 and lectin (Figures 4A, 4B, and S3B). This analysis revealed successful reduction of BEC GLUT1 protein expression by 40% in GLUT-1$^{i\Delta/+BBB}$ mice and 67% in GLUT-1$^{i\Delta BBB}$ mice (Figure 4B). Acutely, partially reducing BEC GLUT1 expression resulted in a profound mortality of GLUT-1$^{i\Delta BBB}$ mice, which all died of seizures within 4 days of tamoxifen-treatment initiation (Figure 4C). On the other hand, reducing BEC GLUT1 expression acutely by 40% in GLUT-1$^{i\Delta/+BBB}$ mice resulted in significant mortality of 50% over a 28-day period following initiation of tamoxifen treatment (Figure 4C). These experiments revealed the profound consequences of even partial, acute downregulation of BEC-GLUT1 expression in adult mice.

When we next compared brain glucose uptake via ^{18}F-FDG PET scans before and after tamoxifen treatment, both

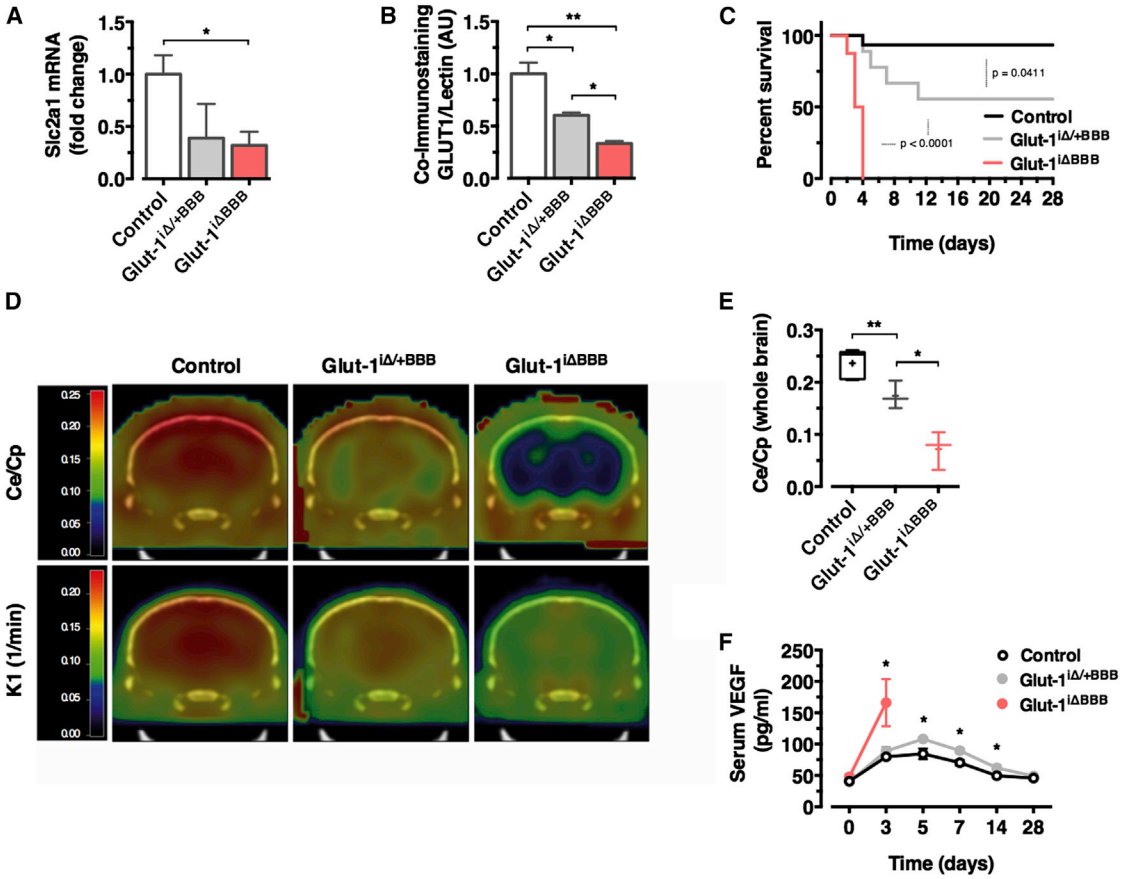

Figure 4. Inducible Deletion of GLUT1 from BECs Reduces Brain Glucose Uptake, Increases Circulating VEGF Concentrations, and Promotes Lethality

(A) qPCR analysis of *Slc2a1* mRNA expression in brains of control mice (n = 5), GLUT-1$^{i\Delta/+BBB}$ mice (n = 3) and GLUT-1$^{i\Delta BBB}$ mice (n = 3), which had been treated with tamoxifen for 3 days.

(B) Confocal microscope analysis of GLUT1 on cortical brain sections of control mice (n = 7), GLUT-1$^{i\Delta/+BBB}$ mice (n = 5) and GLUT-1$^{i\Delta BBB}$ mice (n = 4), which had been treated with tamoxifen for 3 days.

(C) Survival analysis of control mice (n = 15), GLUT-1$^{i\Delta/+BBB}$ mice (n = 9) and GLUT-1$^{i\Delta BBB}$ mice (n = 8), which had been treated with tamoxifen for 3 days.

(D) ^{18}F-FDG PET images of the extracellular brain glucose (C_E)/plasma glucose (C_P) ratio (upper panel) and the unidirectional glucose transport rate K1 (lower panel) in control mice (n = 7), GLUT-1$^{i\Delta/+BBB}$ mice (n = 3) and GLUT-1$^{i\Delta BBB}$ mice (n = 3), which had been treated with tamoxifen for 3 days.

(E) Quantification of whole brain C_E/C_P ratios of control mice (n = 7), GLUT-1$^{i\Delta/+BBB}$ mice (n = 3) and GLUT-1$^{i\Delta BBB}$ mice (n = 3), which had been treated with tamoxifen for 3 days.

(F) Serum VEGF levels of control mice (n = 6), GLUT-1$^{i\Delta/+BBB}$ mice (n = 5) and GLUT-1$^{i\Delta BBB}$ mice (n = 3-5), which had been treated with tamoxifen for 3 days. Results presented as mean ± SEM. *p < 0.05, **p < 0.01, ***p < 0.001.

See also Figure S3.

GLUT-1$^{i\Delta/+BBB}$ mice and GLUT-1$^{i\Delta BBB}$ mice exhibited a dose-dependent reduction of brain glucose uptake (Figures 4D, 4E, S3A, and S3C–S3F). Strikingly, the reduction of brain glucose uptake in GLUT-1$^{i\Delta/+BBB}$ mice was quantitatively comparable to that observed in key glucose sensing regions of mice fed an HFD for 3 days (Figures 2A–2E).

Moreover, longitudinal assessment of serum VEGF concentrations in these animals revealed that in GLUT-1$^{i\Delta BBB}$ mice, after 3 days of tamoxifen treatment, serum VEGF concentrations had increased more than 2-fold compared to tamoxifen-treated control mice (Figure 4F). In GLUT-1$^{i\Delta/+BBB}$ mice, VEGF concentrations significantly increased between 5 and 14 days after initiation of tamoxifen treatment (Figure 4F).

Myeloid-Cell-Derived VEGF Is Required to Maintain BBB-GLUT1 Expression in Obesity

To test whether VEGF upregulation in macrophages is indeed causally required for restoration of BBB-GLUT1 expression and brain glucose metabolism upon prolonged HFD feeding, we decided to investigate the consequence of ablating VEGF expression from myeloid lineage cells on BBB-GLUT1 expression and brain glucose metabolism in obesity. Here, we crossed mice carrying a loxP-flanked *Vegfa* allele (Gerber et al., 1999) with those expressing the Cre-recombinase in myeloid lineage cells under control of the lysozyme(Lys)M-promoter (Clausen et al., 1999). Resulting *Vegfa*$^{lox/lox}$ LysMCre$^{+/-}$, i.e., VEGF$^{\Delta myel}$ mice were then analyzed exposing the animals to either NCD or HFD after

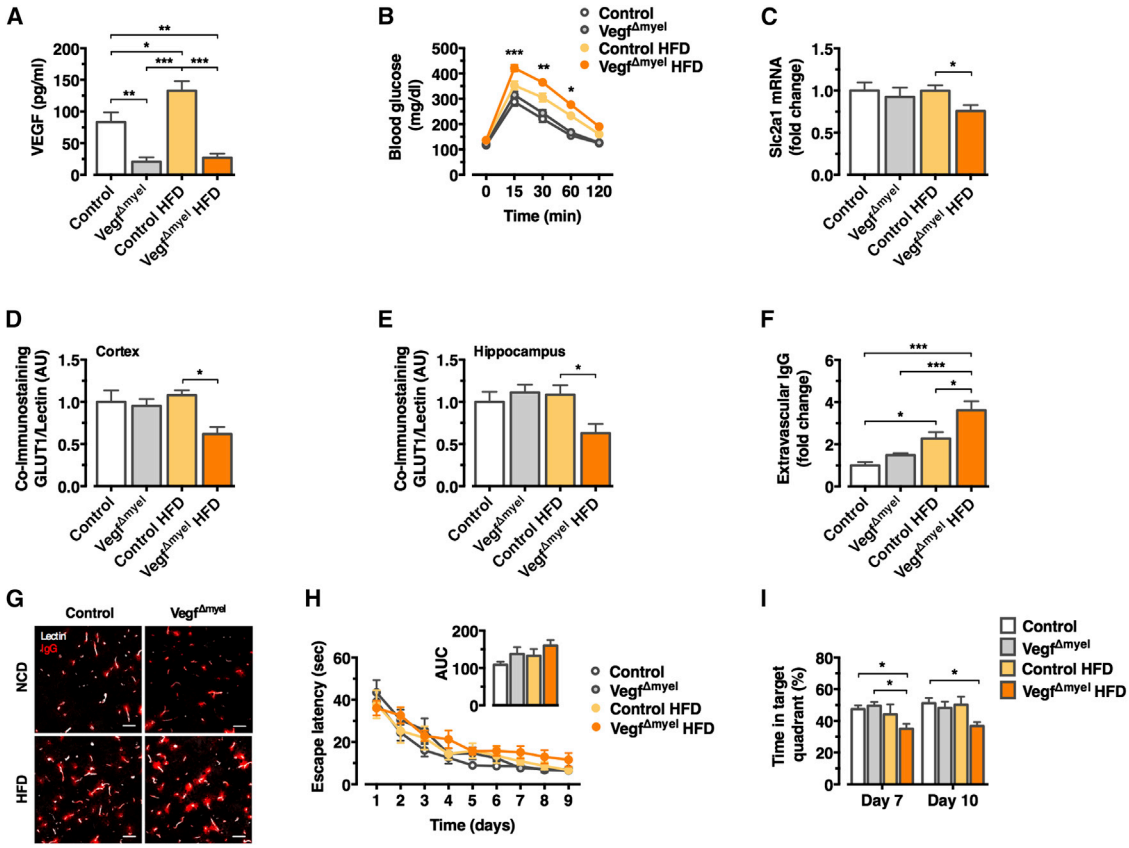

Figure 5. Myeloid-Cell-Derived VEGF Is Required to Maintain Brain Glucose Uptake and Memory Formation in Obesity

(A) Serum VEGF levels in control and VEGF$^{\Delta myel}$ mice, which had been exposed to either NCD (n = 4/5) or HFD (n = 5/8) for 3 months.

(B) Glucose tolerance test in control and VEGF$^{\Delta myel}$ mice, which had been exposed to either NCD (n = 14/17) or HFD (n = 32/37) for 3 months.

(C) qPCR analysis of *Slc2a1* mRNA expression in cortical brain samples of control mice and VEGF$^{\Delta myel}$ mice, which had been exposed to either NCD (n = 6/6) or HFD (n = 12/12) for 6 months.

(D) GLUT1 protein expression in cortical BECs of control mice and VEGF$^{\Delta myel}$ mice, which had been exposed to either NCD (n = 6/4) or HFD (n = 4/6) for 6 months.

(E) GLUT1 protein expression in hippocampal BECs of control mice and VEGF$^{\Delta myel}$ mice, which had been exposed to either NCD (n = 6/4) or HFD (n = 4/4) for 6 months.

(F) Quantification of relative abundance of extravascular IgG in cortical brain samples of control mice and VEGF$^{\Delta myel}$ mice, which had been exposed to either NCD (n = 6/6) or HFD (n = 3/5) for 6 months.

(G) Representative confocal microscopy analysis of relative abundance of extravascular IgG in cortical brain samples of control and VEGF$^{\Delta myel}$ mice on NCD or HFD. Scale bar, 20 μm.

(H) Escape latency during the indicated training days of a Morris water maze task of control and VEGF$^{\Delta myel}$ mice, which had been exposed to either NCD (n = 10/10) or HFD (n = 6/14) for 16 months. Area under the curve (AUC) of escape latencies of the different groups of mice (inset).

(I) Time spent in the target quadrant during retention trials at day 7 and day 10 as described in (H). Data was analyzed using a two-way ANOVA followed by Tuckey's post hoc test.

Results presented as mean ± SEM. *p < 0.05, **p < 0.01, ***p < 0.001.

See also Figure S4.

weaning. Analysis of serum VEGF levels confirmed the increase in circulating VEGF concentrations in control HFD-fed mice compared to NCD-fed controls and revealed a profound reduction in circulating VEGF concentrations in VEGF$^{\Delta myel}$ mice, both on NCD and HFD (Figure 5A). Comparing body weights revealed no significant differences between genotypes, while animals of both genotypes also gained indistinguishably body weight or fat mass upon exposure to HFD, consistent with unaltered steady-state food intake of these animals (Figures S4A–S4C). Similarly, systemic glucose homeostasis remained unaltered in NCD-fed control and VEGF$^{\Delta myel}$ mice as assessed by glucose tolerance testing (Figure 5B). In contrast, HFD-fed VEGF$^{\Delta myel}$ mice exhibited an impaired glucose tolerance compared to control mice, when the animals were exposed to HFD feeding (Figure 5B).

There was no significant difference in *Slc2a1* mRNA expression between control and VEGF$^{\Delta myel}$ mice fed an NCD (Figure 5C), indicating that myeloid-derived VEGF is not required to control BBB-GLUT1 expression in lean mice. However, VEGF$^{\Delta myel}$ mice exhibited significantly reduced *Slc2a1* mRNA expression compared to controls under HFD feeding (Figure 5C). The notion that myeloid-cell-derived VEGF is required for maintenance of BEC-GLUT1 expression under HFD conditions was

further substantiated through co-immunohistochemical staining of GLUT1 in lectin-positive BECs. Here, GLUT1 immunoreactivity remained unaltered in control and VEGF$^{\Delta myel}$ mice under NCD, while VEGF$^{\Delta myel}$ mice exhibited significantly reduced GLUT1 immunoreactivity compared to controls under HFD (Figures 5D, 5E, S4D, and S4E). Consistent with the restoration of BEC GLUT1 expression 4 weeks after HFD feeding, in control animals prolonged HFD feeding did not result in reduced GLUT1 immunoreactivity in BECs, indicating that indeed upregulated VEGF can restore normal BBB-GLUT1 expression upon chronic HFD feeding even in long-term (Figures 5D and 5E).

To directly investigate the consequences of reduced BBB-GLUT1 expression in HFD-fed VEGF$^{\Delta myel}$ mice, we quantified brain glucose uptake in these animals compared to controls exposed to HFD feeding during euglycemic hyperinsulinemic clamps. This analysis revealed a significant reduction of brain glucose uptake in these animals (Figures S4F–S4H). While insulin-stimulated suppression of hepatic glucose production and insulin-stimulated glucose uptake into WAT remained unaltered in these mice, insulin-stimulated glucose uptake into skeletal muscle tended to be increased in VEGF$^{\Delta myel}$ mice, although not reaching statistical significance (Figures S4F–S4H).

Interestingly, we found increased deposits of extravascular immunoglobulin G (IgG) in the cortex of VEGF$^{\Delta myel}$ mice on HFD, but not upon NCD feeding, indicating increased vascular leakage as evidence for altered BBB-permeability in these animals (Figures 5F and 5G).

Given that brain glucose availability is critical for neuronal function, including cognitive performance, we next compared the ability of the different groups of mice at the age of 16 months to properly establish spatial memory in a Morris water maze task. While in lean and obese control mice, as well as in lean VEGF$^{\Delta myel}$ mice, the time required to locate the hidden platform similarly decreased during the training sessions, obese VEGF$^{\Delta myel}$ mice tended to require more time to locate the platform (Figure 5H). Upon removal of the platform, VEGF$^{\Delta myel}$ mice exposed to HFD performed significantly worse to retain spatial memory compared to the NCD-fed groups of mice (Figure 5I).

Myeloid-Cell-Derived VEGF Limits Neurodegeneration in Obesity

In light of the discovery that VEGF is required to maintain brain glucose uptake and cognitive function in obesity, and brain glucose uptake is a critical determinant of the progression of neurodegenerative disorders such as Alzheimer's disease (AD) (Gong et al., 2006; Winkler et al., 2015), we decided to address whether myeloid-cell-derived VEGF is also required to limit neurodegeneration in obesity in a murine AD model. To this end, we crossed VEGF$^{\Delta myel}$ mice with APP.PS1-transgenic mice, expressing the Swedish mutation of amyloid precursor protein (APP) and also expressing a variant of presenilin (PS)-1 (Jankowsky et al., 2004). Further intercrossing of these animals resulted in four different experimental groups of mice, (1) control animals, (2) APP.PS1-transgenic mice, (3) VEGF$^{\Delta myel}$ mice, and (4) VEGF$^{\Delta myel}$ mice, which express the APP.PS1-transgenes.

First, we compared GLUT1 expression in BECs in the different lines of animals both in cortex and hippocampus. Consistent with what we observed in VEGF$^{\Delta myel}$ mice compared to controls on NCD, lean VEGF$^{\Delta myel}$ mice generated from these intercrosses exhibited unaltered GLUT1 expression in BECs (Figures S5A–S5D). APP.PS1-transgenic mice exhibited unaltered BBB-GLUT1 expression under NCD and this remained unchanged in the additional absence of myeloid-cell-derived VEGF in lean VEGF$^{\Delta myel}$/APP.PS1 mice (Figures S5A–S5D).

Upon HFD feeding, however, mRNA and protein expression of BBB-GLUT1 expression decreased to similar extent in both VEGF$^{\Delta myel}$ and VEGF$^{\Delta myel}$/APP.PS1 mice in cortex (Figures 6A, 6B, and 6D) as well as BBB-GLUT1 protein expression decreased in hippocampus (Figures 6C and 6E).

Since cognitive deficits have been reported to manifest at the age of 9 months in APP.PS1-transgenic mice (Jankowsky et al., 2004), we aimed to test, whether impairment of brain glucose uptake in HFD-fed VEGF$^{\Delta myel}$/APP.PS1 mice could aggravate this phenotype and therefore assessed spatial memory learning in 6-month-old mice. Indeed, already at this young age only VEGF$^{\Delta myel}$/APP.PS1 mice, when exposed to HFD, performed significantly worse compared to all other tested genotypes (Figures 6F and 6G). These data indicate that HFD feeding in the presence of reduced circulating VEGF concentrations aggravates cognitive defects in APP.PS1-transgenic mice.

Next, we aimed to investigate the molecular basis for aggravated memory impairment of VEGF$^{\Delta myel}$/APP.PS1 mice and therefore quantified amyloid plaque burden in the different groups of mice. While plaque burden was significantly increased in the presence of the APP.PS1-transgene, Aβ-plaque formation was not further aggravated in the absence of myeloid-cell-derived VEGF both in NCD- and HFD-fed animals (Figures 7A, 7B, S6A, and S6B). Similarly, brain levels of Aβ_{1-42} as assessed by ELISA detection remained unaltered in the absence of myeloid-derived VEGF in APP.PS1-transgenic mice (Figure S6C). Thus, impairing brain glucose metabolism on an AD background does not aggravate plaque formation.

To study the underlying mechanism by which the absence of myeloid-derived VEGF impaired cognitive function in APP.PS1-transgenic mice, vascular leakage was assessed by quantification of extravascular accumulation of IgG. This analysis confirmed a significant increase in IgG deposits in the absence of myeloid-derived VEGF as an additional evidence of altered BBB functionality in these obese mice (Figures 7C and 7D).

Another hallmark in AD progression is the activation of neuroinflammation. Thus, we determined the distribution of GFAP immunoreactivity as readout for astrocyte activation in the brains of the different animals. This analysis revealed that in APP.PS1-transgenic animals, the number of GFAP-immunoreactive cells clearly increased both in cortex and hippocampus (Figures 7E, 7F, S7A, and S7B). However, under HFD feeding conditions, the additional absence of myeloid-derived VEGF and thus subsequently reduced brain glucose uptake caused a further significant increase in GFAP immunoreactivity in HFD-fed VEGF$^{\Delta myel}$/APP.PS1 mice (Figures 7E, 7F, S7A, and S7B). In addition, immunoreactivity of phosphorylated c-Jun (p-c-Jun) as readout for inflammatory JNK-activation was further substantially increased under these conditions in HFD-fed VEGF$^{\Delta myel}$/APP.PS1 mice (Figures 7G, 7H, S7C, and S7D).

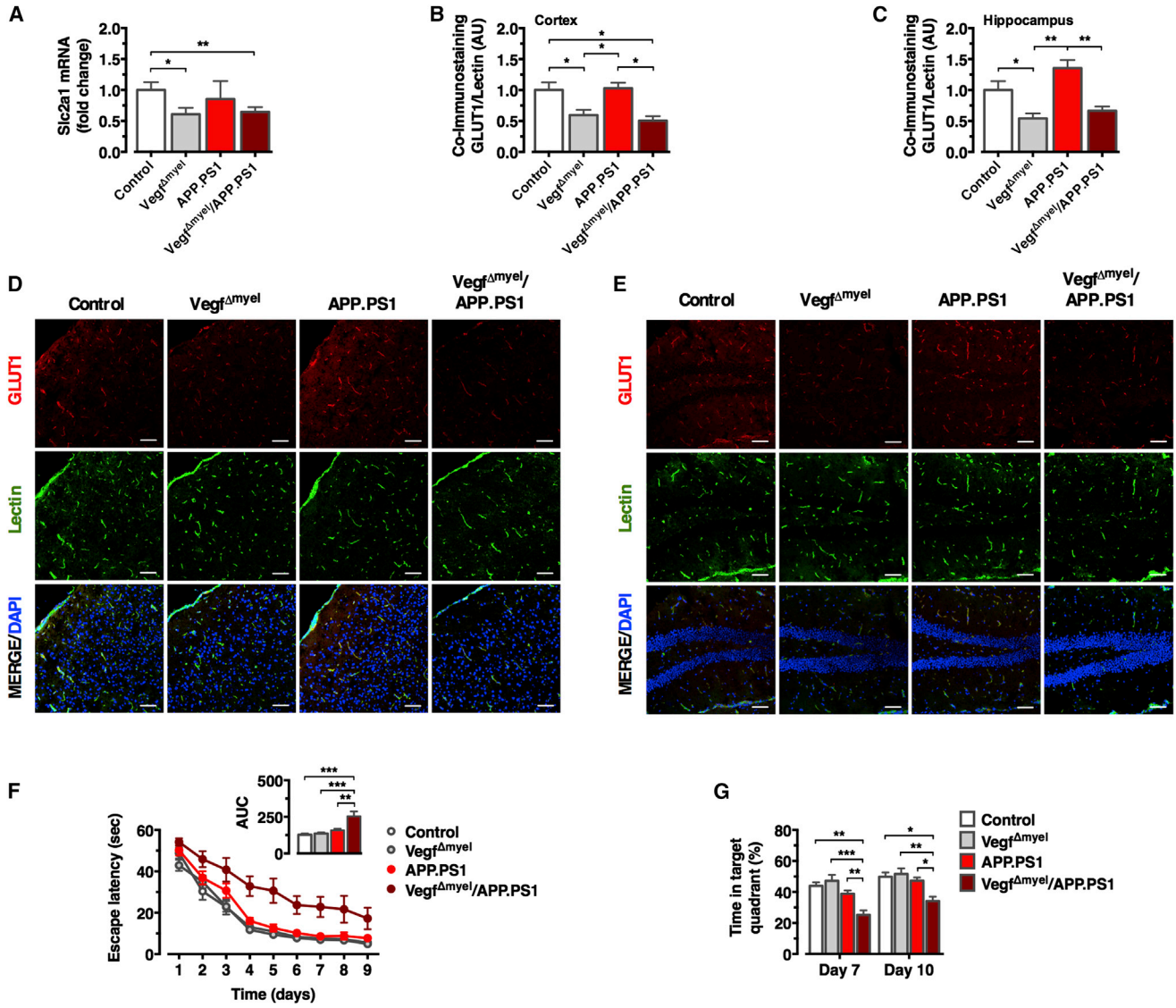

Figure 6. Myeloid-Cell-Derived VEGF Limits Memory Loss in Obese APP.PS1-Transgenic Mice

(A) qPCR analysis of *Slc2a1* mRNA expression in cortical brain samples of in HFD-fed control mice, VEGF$^{\Delta myel}$ mice, APP.PS1 mice and VEGF$^{\Delta myel}$/APP.PS1 mice at the age of 6 months. n = 5 per group.

(B and C) GLUT1 protein expression in BECs of cortex (B) and hippocampus (C) in HFD-fed control mice (n = 9), VEGF$^{\Delta myel}$ mice (n = 8), APP.PS1 mice (n = 9), and VEGF$^{\Delta myel}$/APP.PS1 mice (n = 10) at the age of 6 months.

(D and E) Representative confocal microscopy analysis of GLUT1 protein expression in BECs of cortex (D) and hippocampus (E). Scale bar, 100 μm.

(F) Escape latency during the indicated training days of a Morris water maze task of HFD-fed control mice (n = 12), VEGF$^{\Delta myel}$ mice (n = 17), APP.PS1 mice (n = 14), and VEGF$^{\Delta myel}$/APP.PS1 mice (n = 10) at the age of 6 months. Area under the curve (AUC) of escape latencies of the different groups of mice (inset).

(G) Time spent in the target quadrant during retention trials at day 7 and day 10 as described in (F).

Results presented as mean ± SEM. *p < 0.05, **p < 0.01, ***p < 0.001.

See also Figure S5.

Taken together, reducing brain glucose uptake through HFD feeding and simultaneously preventing the compensatory increase in circulating VEGF cooperates with APP.PS1-driven neurodegeneration through aggravation of neuroinflammation without increasing Aβ_{1-42} processing or plaque burden. Thus, circulating VEGF is also critically required to limit AD-associated cognitive impairment and progression of neuroinflammation in obesity.

DISCUSSION

We demonstrate that acute HFD feeding in mice transiently reduces GLUT1 expression in vascular endothelial cells of the BBB (BECs) and functionally reduces brain glucose uptake. This finding is further substantiated by the notion that incubation of BECs with serum derived from mice exposed to high-fat diet

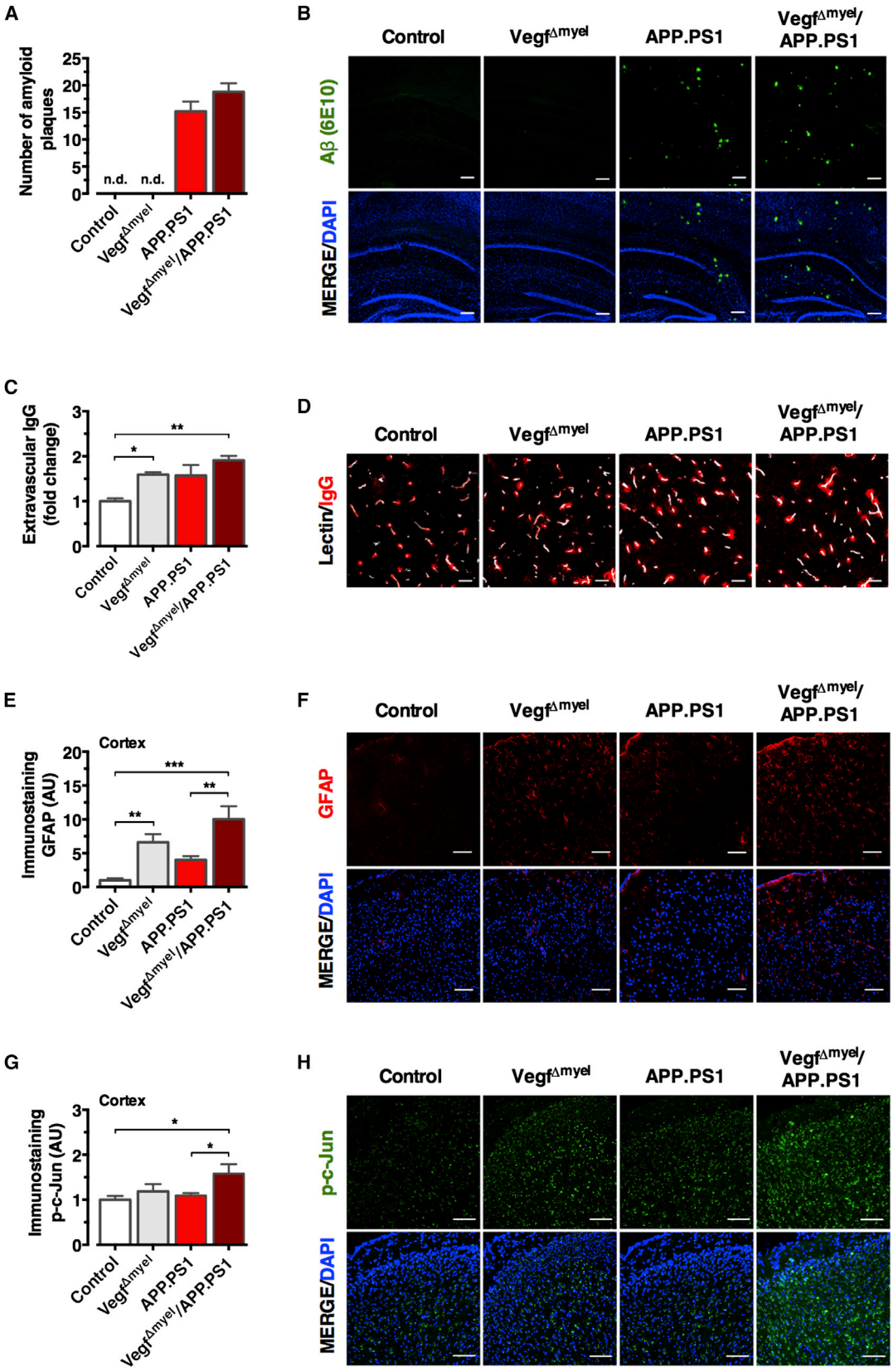

(legend on next page)

feeding for 3 days significantly reduces GLUT1 mRNA and protein expression. This clearly indicates the presence of soluble factor(s) in serum of these animals, which are responsible for reducing GLUT1 expression in BECs. We also demonstrate that palmitic acid as a saturated fatty acid, which is increased in circulation of obese mice (Benoit et al., 2009; Boden, 1997), acutely inhibits glucose uptake and glycolytic metabolism in cultured BECs. Thus, saturated fatty acids may provide an interesting candidate to mediate BBB-GLUT1 downregulation in obesity. However, the exact nature of these signal(s) and the molecular mechanisms activated to decrease GLUT1 expression in BECs remains to be identified in further studies.

Another important question is how transiently lowered brain glucose uptake leads to increased circulating VEGF concentrations and ultimately to restored BBB-GLUT1 expression. Our experiments reveal that the primary source of compensatory VEGF production in obesity is myeloid lineage cells, likely CD206-positive perivascular macrophages. Although a minor component of the CNS, perivascular macrophages are important immunoregulatory cells (Galea et al., 2005; Williams et al., 2001). These cells appear to account for the majority of increased VEGF during the first 4 weeks of HFD feeding, when no persistent increases of VEGF expression in spleen, liver, and adipose tissue are detectable. It appears likely that during the further course of obesity development, macrophages recruited to adipose tissue may also contribute to the compensatory increase in circulating VEGF concentrations. This notion is consistent with the previous reports of elevated VEGF release from visceral adipose tissue of obese subjects (Schlich et al., 2013).

Future experiments will have to delineate how reduced brain glucose uptake couples to activation of perivascular macrophages to increase VEGF production and ultimately re-instate GLUT1 expression at the neurovascular unit. One possibility is that glucose-sensitive neurons, which respond to changes in extracellular glucose concentration (Steinbusch et al., 2015), can regulate parasympathetic outflow, which in turn activates inflammation. The reduction of brain glucose uptake reported here on acute HFD feeding is particularly predominant in areas that are enriched in glucose-sensing neurons such as the hypothalamus (Karschin et al., 1997; Levin et al., 1999; Peters et al., 2004). Reduction of parasympathetic tone is well documented in obesity and has been demonstrated to contribute to the activation of inflammation of obesity (Andersson and Tracey, 2012; Rosas-Ballina and Tracey, 2009). In fact, specific activation of parasympathetic α7-nicotinergic receptors can limit obesity-induced inflammation and improve obesity-associated systemic insulin resistance (Bencherif et al., 2011; Wang et al., 2011). Clearly, further studies have to define the neurocircuitry, which couples reduced neuronal glucose availability to the activation of VEGF production in macrophages, both in the BBB and in other tissues.

Given the critical role of tight control of brain glucose availability for organismal survival, activation of VEGF expression and inflammation upon transient reduction of brain glucose metabolism provides a prime mechanism to reinstate glucose availability to the CNS. First, increased VEGF concentrations can restore glucose uptake in BECs, as shown here in vitro and in vivo. Second, activation of systemic inflammation causes insulin resistance in skeletal muscle and adipose tissue (Sabio et al., 2008), thereby reducing insulin-stimulated glucose uptake in these tissues and impairing insulin-stimulated suppression of hepatic glucose production (Arkan et al., 2005; Sabio et al., 2008; Wunderlich et al., 2008). Thus, blood glucose concentrations increase and thereby provide increased substrate availability for the CNS. This concept would define obesity-associated inflammation as a homeostatic regulatory principle to restore transiently decreased brain glucose uptake in obesity through multiple mechanisms.

The notion that activation of inflammatory signaling represents a key step in the development of obesity-associated insulin resistance has fueled a whole research area to identify anti-inflammatory strategies as novel drug targets for this disease (Gregor and Hotamisligil, 2011; Hotamisligil, 2006). However, currently the efficiency of anti-inflammatory strategies is solely assessed based on their ability to improve peripheral insulin sensitivity and glucose metabolism. Thus, when inflammatory signaling pathways are targeted in metabolic diseases, attention will have to be paid to the potential side effects of the intervention on compensatory VEGF production and its potential detrimental effects on brain glucose metabolism, cognition, and neurodegeneration.

Finally, our results may have clear implications for further strategies targeting neurodegenerative disorders such as AD. Recent studies have revealed a critical role for brain glucose metabolism in AD progression. On the one hand, glucose availability has been implicated in the activity-dependent co-secretion of Aβ-peptides and thus contributes to activity-dependent progression of neurodegeneration (Macauley et al., 2015). On the other hand, it was demonstrated that partially reducing BBB-GLUT1 expression leads to massive progression of AD pathology in mouse models (Winkler et al., 2015). Interestingly, the latter phenomenon occurred in the absence of alterations in Aβ-processing and accumulation, similar to what is observed in our VEGF$^{\Delta myel}$/APP.PS1 mice under high-fat diet conditions.

Figure 7. Myeloid-Cell-Derived VEGF Limits Neuroinflammation in Obese APP.PS1-Transgenic Mice

(A and B) Immunohistochemical assessment of Aβ_{1-42}-immunoreative plaques in HFD-fed control mice (n = 10), VEGF$^{\Delta myel}$ mice (n = 10), APP.PS1 mice (n = 10), and VEGF$^{\Delta myel}$/APP.PS1 mice (n = 10) at the age of 6 months. Scale bar, 100 μm.

(C and D) Quantification and representative confocal microscopy analysis of relative abundance of extravascular IgG in cortical brain samples of HFD-fed control mice (n = 4), VEGF$^{\Delta myel}$ mice (n = 5), APP.PS1 mice (n = 5), and VEGF$^{\Delta myel}$/APP.PS1 mice (n = 5) at the age of 6 months. Scale bar, 20 μm.

(E and F) Immunohistochemical assessment of GFAP-positive astrocytes in HFD-fed control mice (n = 9), VEGF$^{\Delta myel}$ mice (n = 7), APP.PS1 mice (n = 10), and VEGF$^{\Delta myel}$/APP.PS1 mice (n = 8) at the age of 6 months. Scale bar, 100 μm.

(G and H) Immunohistochemical assessment of p-c-Jun-positive cells in brains of HFD-fed control mice (n = 3), VEGF$^{\Delta myel}$ mice (n = 6), APP.PS1 mice (n = 6), and VEGF$^{\Delta myel}$/APP.PS1 mice (n = 5) at the age of 6 months. Scale bar, 100 μm.

Results presented as mean ± SEM. *p < 0.05, **p < 0.01, ***p < 0.001.

See also Figures S6 and S7.

Collectively, our study assigns VEGF a critical compensatory role to reinstate brain glucose metabolism in obesity, a notion of far-reaching therapeutic implications not only for obesity, but also cancer treatment and that of neurodegenerative disorders in obese subjects, setting the ground for more personalized therapeutic decisions in obese patients in the future.

EXPERIMENTAL PROCEDURES

Animal Husbandry

All animal procedures were conducted in compliance with protocols approved by local government authorities (Bezirksregierung Köln) and were in accordance with NIH guidelines. Mice were housed in groups of three to five at 22°C–24°C using a 12 hr light/12 hr dark cycle. Animals had ad libitum access to water at all times, and food was only withdrawn if required for an experiment. All mouse models are described in the Supplemental Experimental Procedures.

Indirect Calorimetry

Indirect calorimetry measurements were performed as described in the Supplemental Experimental Procedures.

Immunohistochemistry

Immunohistochemistry was performed as described in the Supplemental Experimental Procedures.

PET Imaging

PET imaging was performed using an Inveon preclinical PET/CT system (Siemens) as described in the Supplemental Experimental Procedures.

Culture of Cerebral Endothelial Cells

The immortalized mouse brain capillary EC line cerebral endothelial cells (cEND) were used as described (Förster et al., 2005) and outlined in the Supplemental Experimental Procedures.

Glucose Uptake Assay

Cellular glucose uptake was measured in cEND cells using a fluorescent 2-NBDG assay. For details, refer to the Supplemental Experimental Procedures.

Measurement of Glycolytic Flux

Extracellular acidification rate (ECAR) was measured using the XF96 Flux Analyzer (Seahorse Bioscience). For details, see Supplemental Experimental Procedures.

Glucose Tolerance Test

Glucose tolerance tests were performed as previously described in (Tovar et al., 2013) and as outlined in the Supplemental Experimental Procedures.

Hyperinsulinemic-Euglycemic Clamp Studies in Awake Mice

Clamp experiments were performed as outlined in the Supplemental Experimental Procedures.

Morris Water Maze

The Morris water maze was used to test spatial learning and to evaluate the working and reference memory functions. Lean or obese $VEGF^{\Delta myel}$ mice and control mice were tested at 16 months of age. Obese HFD-fed APP.PS1-transgenic mice, $VEGF^{\Delta myel}$ mice, $VEGF^{\Delta myel}$/APP.PS1 mice, and corresponding controls were tested at 6 months of age. For details see the Supplemental Experimental Procedures.

Statistical Analyses

All data, unless otherwise indicated, are shown as mean values ± SEM. In boxplots, the upper and lower whiskers indicate the minimum and maximum values of the data, center lines indicate the median, and the mean values are represented by plus signs. Datasets with only two independent groups were analyzed for statistical significance using unpaired two-tailed Student's t test. Datasets with more than two groups were analyzed using either one-way ANOVA followed by Tukey's post hoc test or two-way ANOVA followed by Tukey's post hoc test. For statistical analyses of GTTs, we performed two-way ANOVAs followed by Bonferroni's post hoc test. All figures and statistical analyses were generated using GraphPad Prism 6. $p < 0.05$ was considered to indicate statistical significance.

Other Methods

See the Supplemental Experimental Procedures.

SUPPLEMENTAL INFORMATION

Supplemental Information includes Supplemental Experimental Procedures and seven figures and can be found with this article online at http://dx.doi.org/10.1016/j.cell.2016.03.033.

AUTHOR CONTRIBUTIONS

Conceptualization, J.C.B., M.S., and A.J.; Methodology, J.C.B., M.S., A.J., H.B., and B.C.; Formal Analysis, Investigation, and Visualization, M.S., A.J., H.B., B.C., S.T., A.K., J.M., S.M.S., B.H., J.G., and J.A.; Writing – Original Draft, J.C.B. and A.J.; Writing – Review & Editing, J.C.B, M.S., and A.J.; Supervision, Resources, and Funding Acquisition, J.C.B., C.Y.F., S.A.E., M.S., N.F., and G.K.

ACKNOWLEDGMENTS

This work was supported by a grant from the DFG (BR 1492/7-1) to J.C.B., and received funding by the DFG within the framework of the TRR134 and within the CMMC and the Excellence Initiative by German Federal and State Governments (CECAD). This work was funded (in part) by the Helmholtz Alliance ICEMED (Imaging and Curing Environmental Metabolic Diseases) through the Initiative and Networking Fund of the Helmholtz Association. Moreover, the research leading to these results has received funding from the European Union Seventh Framework Program (FP7/2007-2013) under grant agreement 266408. S.M.S. was funded by the Humboldt-Bayer program of the Alexander Von Humboldt foundation and received a grant from the Excellence Cluster on Cellular Stress Responses in Aging Associated Diseases (CECAD). A.K. was supported by a DFG fellowship KL2399-3/1. S.T. was funded by a scholarship-program (Gerok-Rotationsstelle, No. 3/2014) of the Medical Faculty of the University of Cologne. G.K. was funded by the National Institute on Aging (NIA) grant 1R01DK104727-01A1. [18F]FDG was provided by B. Neumaier and the radiochemistry department of the Max Planck Institute for Metabolism Research.

Received: August 27, 2015
Revised: January 25, 2016
Accepted: March 16, 2016
Published: April 28, 2016

REFERENCES

Andersson, U., and Tracey, K.J. (2012). Reflex principles of immunological homeostasis. Annu. Rev. Immunol. *30*, 313–335.

Arkan, M.C., Hevener, A.L., Greten, F.R., Maeda, S., Li, Z.W., Long, J.M., Wynshaw-Boris, A., Poli, G., Olefsky, J., and Karin, M. (2005). IKK-beta links inflammation to obesity-induced insulin resistance. Nat. Med. *11*, 191–198.

Bencherif, M., Lippiello, P.M., Lucas, R., and Marrero, M.B. (2011). Alpha7 nicotinic receptors as novel therapeutic targets for inflammation-based diseases. Cell. Mol. Life Sci. *68*, 931–949.

Benoit, S.C., Kemp, C.J., Elias, C.F., Abplanalp, W., Herman, J.P., Migrenne, S., Lefevre, A.L., Cruciani-Guglielmacci, C., Magnan, C., Yu, F., et al. (2009). Palmitic acid mediates hypothalamic insulin resistance by altering PKC-theta subcellular localization in rodents. J. Clin. Invest. *119*, 2577–2589.

Boden, G. (1997). Role of fatty acids in the pathogenesis of insulin resistance and NIDDM. Diabetes *46*, 3–10.

Clausen, B.E., Burkhardt, C., Reith, W., Renkawitz, R., and Förster, I. (1999). Conditional gene targeting in macrophages and granulocytes using LysMcre mice. Transgenic Res. *8*, 265–277.

De Vivo, D.C., Trifiletti, R.R., Jacobson, R.I., Ronen, G.M., Behmand, R.A., and Harik, S.I. (1991). Defective glucose transport across the blood-brain barrier as a cause of persistent hypoglycorrhachia, seizures, and developmental delay. N. Engl. J. Med. *325*, 703–709.

Förster, C., Silwedel, C., Golenhofen, N., Burek, M., Kietz, S., Mankertz, J., and Drenckhahn, D. (2005). Occludin as direct target for glucocorticoid-induced improvement of blood-brain barrier properties in a murine in vitro system. J. Physiol. *565*, 475–486.

Freemerman, A.J., Johnson, A.R., Sacks, G.N., Milner, J.J., Kirk, E.L., Troester, M.A., Macintyre, A.N., Goraksha-Hicks, P., Rathmell, J.C., and Makowski, L. (2014). Metabolic reprogramming of macrophages: glucose transporter 1 (GLUT1)-mediated glucose metabolism drives a proinflammatory phenotype. J. Biol. Chem. *289*, 7884–7896.

Galea, I., Palin, K., Newman, T.A., Van Rooijen, N., Perry, V.H., and Boche, D. (2005). Mannose receptor expression specifically reveals perivascular macrophages in normal, injured, and diseased mouse brain. Glia *49*, 375–384.

Gautron, L., Elmquist, J.K., and Williams, K.W. (2015). Neural control of energy balance: translating circuits to therapies. Cell *161*, 133–145.

Gerber, H.P., Hillan, K.J., Ryan, A.M., Kowalski, J., Keller, G.A., Rangell, L., Wright, B.D., Radtke, F., Aguet, M., and Ferrara, N. (1999). VEGF is required for growth and survival in neonatal mice. Development *126*, 1149–1159.

Gong, C.X., Liu, F., Grundke-Iqbal, I., and Iqbal, K. (2006). Impaired brain glucose metabolism leads to Alzheimer neurofibrillary degeneration through a decrease in tau O-GlcNAcylation. J. Alzheimers Dis. *9*, 1–12.

Gregor, M.F., and Hotamisligil, G.S. (2011). Inflammatory mechanisms in obesity. Annu. Rev. Immunol. *29*, 415–445.

He, H., Xu, J., Warren, C.M., Duan, D., Li, X., Wu, L., and Iruela-Arispe, M.L. (2012). Endothelial cells provide an instructive niche for the differentiation and functional polarization of M2-like macrophages. Blood *120*, 3152–3162.

Heilig, C., Brosius, F., Siu, B., Concepcion, L., Mortensen, R., Heilig, K., Zhu, M., Weldon, R., Wu, G., and Conner, D. (2003). Implications of glucose transporter protein type 1 (GLUT1)-haplodeficiency in embryonic stem cells for their survival in response to hypoxic stress. Am. J. Pathol. *163*, 1873–1885.

Horwood, N., and Davies, D.C. (1994). Immunolabelling of hippocampal microvessel glucose transporter protein is reduced in Alzheimer's disease. Virchows Arch. *425*, 69–72.

Hotamisligil, G.S. (2006). Inflammation and metabolic disorders. Nature *444*, 860–867.

Jankowsky, J.L., Fadale, D.J., Anderson, J., Xu, G.M., Gonzales, V., Jenkins, N.A., Copeland, N.G., Lee, M.K., Younkin, L.H., Wagner, S.L., et al. (2004). Mutant presenilins specifically elevate the levels of the 42 residue beta-amyloid peptide in vivo: evidence for augmentation of a 42-specific gamma secretase. Hum. Mol. Genet. *13*, 159–170.

Kalaria, R.N., and Harik, S.I. (1989). Reduced glucose transporter at the blood-brain barrier and in cerebral cortex in Alzheimer disease. J. Neurochem. *53*, 1083–1088.

Kälin, S., Heppner, F.L., Bechmann, I., Prinz, M., Tschöp, M.H., and Yi, C.X. (2015). Hypothalamic innate immune reaction in obesity. Nat. Rev. Endocrinol. *11*, 339–351.

Karschin, C., Ecke, C., Ashcroft, F.M., and Karschin, A. (1997). Overlapping distribution of K(ATP) channel-forming Kir6.2 subunit and the sulfonylurea receptor SUR1 in rodent brain. FEBS Lett. *401*, 59–64.

Kleinridders, A., Könner, A.C., and Brüning, J.C. (2009a). CNS-targets in control of energy and glucose homeostasis. Curr. Opin. Pharmacol. *9*, 794–804.

Kleinridders, A., Schenten, D., Könner, A.C., Belgardt, B.F., Mauer, J., Okamura, T., Wunderlich, F.T., Medzhitov, R., and Brüning, J.C. (2009b). MyD88 signaling in the CNS is required for development of fatty acid-induced leptin resistance and diet-induced obesity. Cell Metab. *10*, 249–259.

Lee, S., Chen, T.T., Barber, C.L., Jordan, M.C., Murdock, J., Desai, S., Ferrara, N., Nagy, A., Roos, K.P., and Iruela-Arispe, M.L. (2007). Autocrine VEGF signaling is required for vascular homeostasis. Cell *130*, 691–703.

Lee, Y.S., Li, P., Huh, J.Y., Hwang, I.J., Lu, M., Kim, J.I., Ham, M., Talukdar, S., Chen, A., Lu, W.J., et al. (2011). Inflammation is necessary for long-term but not short-term high-fat diet-induced insulin resistance. Diabetes *60*, 2474–2483.

Levin, B.E., Dunn-Meynell, A.A., and Routh, V.H. (1999). Brain glucose sensing and body energy homeostasis: role in obesity and diabetes. Am. J. Physiol. *276*, R1223–R1231.

Macauley, S.L., Stanley, M., Caesar, E.E., Yamada, S.A., Raichle, M.E., Perez, R., Mahan, T.E., Sutphen, C.L., and Holtzman, D.M. (2015). Hyperglycemia modulates extracellular amyloid-β concentrations and neuronal activity in vivo. J. Clin. Invest. *125*, 2463–2467.

Macintyre, A.N., Gerriets, V.A., Nichols, A.G., Michalek, R.D., Rudolph, M.C., Deoliveira, D., Anderson, S.M., Abel, E.D., Chen, B.J., Hale, L.P., and Rathmell, J.C. (2014). The glucose transporter Glut1 is selectively essential for CD4 T cell activation and effector function. Cell Metab. *20*, 61–72.

Mani, N., Khaibullina, A., Krum, J.M., and Rosenstein, J.M. (2003). Activation of receptor-mediated angiogenesis and signaling pathways after VEGF administration in fetal rat CNS explants. J. Cereb. Blood Flow Metab. *23*, 1420–1429.

Mooradian, A.D., Chung, H.C., and Shah, G.N. (1997). GLUT-1 expression in the cerebra of patients with Alzheimer's disease. Neurobiol. Aging *18*, 469–474.

Pekala, P., Marlow, M., Heuvelman, D., and Connolly, D. (1990). Regulation of hexose transport in aortic endothelial cells by vascular permeability factor and tumor necrosis factor-alpha, but not by insulin. J. Biol. Chem. *265*, 18051–18054.

Peters, A., Schweiger, U., Pellerin, L., Hubold, C., Oltmanns, K.M., Conrad, M., Schultes, B., Born, J., and Fehm, H.L. (2004). The selfish brain: competition for energy resources. Neurosci. Biobehav. Rev. *28*, 143–180.

Ridder, D.A., Lang, M.F., Salinin, S., Röderer, J.P., Struss, M., Maser-Gluth, C., and Schwaninger, M. (2011). TAK1 in brain endothelial cells mediates fever and lethargy. J. Exp. Med. *208*, 2615–2623.

Rosas-Ballina, M., and Tracey, K.J. (2009). The neurology of the immune system: neural reflexes regulate immunity. Neuron *64*, 28–32.

Sabio, G., Das, M., Mora, A., Zhang, Z., Jun, J.Y., Ko, H.J., Barrett, T., Kim, J.K., and Davis, R.J. (2008). A stress signaling pathway in adipose tissue regulates hepatic insulin resistance. Science *322*, 1539–1543.

Schlich, R., Willems, M., Greulich, S., Ruppe, F., Knoefel, W.T., Ouwens, D.M., Maxhera, B., Lichtenberg, A., Eckel, J., and Sell, H. (2013). VEGF in the crosstalk between human adipocytes and smooth muscle cells: depot-specific release from visceral and perivascular adipose tissue. Mediators Inflamm. *2013*, 982458.

Seidner, G., Alvarez, M.G., Yeh, J.I., O'Driscoll, K.R., Klepper, J., Stump, T.S., Wang, D., Spinner, N.B., Birnbaum, M.J., and De Vivo, D.C. (1998). GLUT-1 deficiency syndrome caused by haploinsufficiency of the blood-brain barrier hexose carrier. Nat. Genet. *18*, 188–191.

Sone, H., Deo, B.K., and Kumagai, A.K. (2000). Enhancement of glucose transport by vascular endothelial growth factor in retinal endothelial cells. Invest. Ophthalmol. Vis. Sci. *41*, 1876–1884.

Steinbusch, L., Labouèbe, G., and Thorens, B. (2015). Brain glucose sensing in homeostatic and hedonic regulation. Trends Endocrinol. Metab. *26*, 455–466.

Takata, K., Kasahara, T., Kasahara, M., Ezaki, O., and Hirano, H. (1990). Erythrocyte/HepG2-type glucose transporter is concentrated in cells of blood-tissue barriers. Biochem. Biophys. Res. Commun. *173*, 67–73.

Thaler, J.P., Yi, C.X., Schur, E.A., Guyenet, S.J., Hwang, B.H., Dietrich, M.O., Zhao, X., Sarruf, D.A., Izgur, V., Maravilla, K.R., et al. (2012). Obesity is associated with hypothalamic injury in rodents and humans. J. Clin. Invest. *122*, 153–162.

Tovar, S., Paeger, L., Hess, S., Morgan, D.A., Hausen, A.C., Brönneke, H.S., Hampel, B., Ackermann, P.J., Evers, N., Büning, H., et al. (2013). K(ATP)-channel-dependent regulation of catecholaminergic neurons controls BAT sympathetic nerve activity and energy homeostasis. Cell Metab. *18*, 445–455.

Tsaousidou, E., Paeger, L., Belgardt, B.F., Pal, M., Wunderlich, C.M., Brönneke, H., Collienne, U., Hampel, B., Wunderlich, F.T., Schmidt-Supprian, M., et al. (2014). Distinct roles for JNK and IKK activation in Agouti-related peptide neurons in the development of obesity and insulin resistance. Cell Rep. *9*, 1495–1506.

Vannucci, S.J., Maher, F., Koehler, E., and Simpson, I.A. (1994). Altered expression of GLUT-1 and GLUT-3 glucose transporters in neurohypophysis of water-deprived or diabetic rats. Am. J. Physiol. *267*, E605–E611.

Vogt, M.C., and Brüning, J.C. (2013). CNS insulin signaling in the control of energy homeostasis and glucose metabolism - from embryo to old age. Trends Endocrinol. Metab. *24*, 76–84.

Wang, D., Pascual, J.M., Yang, H., Engelstad, K., Mao, X., Cheng, J., Yoo, J., Noebels, J.L., and De Vivo, D.C. (2006). A mouse model for Glut-1 haploinsufficiency. Hum. Mol. Genet. *15*, 1169–1179.

Wang, X., Yang, Z., Xue, B., and Shi, H. (2011). Activation of the cholinergic antiinflammatory pathway ameliorates obesity-induced inflammation and insulin resistance. Endocrinology *152*, 836–846.

Wei, J., Shimazu, J., Makinistoglu, M.P., Maurizi, A., Kajimura, D., Zong, H., Takarada, T., Iezaki, T., Pessin, J.E., Hinoi, E., and Karsenty, G. (2015). Glucose uptake and Runx2 synergize to orchestrate osteoblast differentiation and bone formation. Cell *161*, 1576–1591.

Williams, K.W., and Elmquist, J.K. (2012). From neuroanatomy to behavior: central integration of peripheral signals regulating feeding behavior. Nat. Neurosci. *15*, 1350–1355.

Williams, K., Alvarez, X., and Lackner, A.A. (2001). Central nervous system perivascular cells are immunoregulatory cells that connect the CNS with the peripheral immune system. Glia *36*, 156–164.

Winkler, E.A., Nishida, Y., Sagare, A.P., Rege, S.V., Bell, R.D., Perlmutter, D., Sengillo, J.D., Hillman, S., Kong, P., Nelson, A.R., et al. (2015). GLUT1 reductions exacerbate Alzheimer's disease vasculo-neuronal dysfunction and degeneration. Nat. Neurosci. *18*, 521–530.

Wunderlich, F.T., Luedde, T., Singer, S., Schmidt-Supprian, M., Baumgartl, J., Schirmacher, P., Pasparakis, M., and Brüning, J.C. (2008). Hepatic NF-kappa B essential modulator deficiency prevents obesity-induced insulin resistance but synergizes with high-fat feeding in tumorigenesis. Proc. Natl. Acad. Sci. USA *105*, 1297–1302.

Yeh, W.L., Lin, C.J., and Fu, W.M. (2008). Enhancement of glucose transporter expression of brain endothelial cells by vascular endothelial growth factor derived from glioma exposed to hypoxia. Mol. Pharmacol. *73*, 170–177.

Yi, C.X., Gericke, M., Krüger, M., Alkemade, A., Kabra, D.G., Hanske, S., Filosa, J., Pfluger, P., Bingham, N., Woods, S.C., et al. (2012a). High calorie diet triggers hypothalamic angiopathy. Mol. Metab. *1*, 95–100.

Yi, C.X., Tschöp, M.H., Woods, S.C., and Hofmann, S.M. (2012b). High-fat-diet exposure induces IgG accumulation in hypothalamic microglia. Dis. Model. Mech. *5*, 686–690.

Zhang, Y., Proenca, R., Maffei, M., Barone, M., Leopold, L., and Friedman, J.M. (1994). Positional cloning of the mouse obese gene and its human homologue. Nature *372*, 425–432.